A bead-based activity screen for small-molecule inhibitors of signal transduction in chronic myelogenous leukemia cells

*Juliesta E. Sylvester †§ and Stephen J. Kron *‡§*

† Department of Biochemistry and Molecular Biology, ‡ Department of Molecular Genetics and Cell Biology, and § the Ludwig Center for Metastasis Research, The University of Chicago, Chicago, Illinois 60637

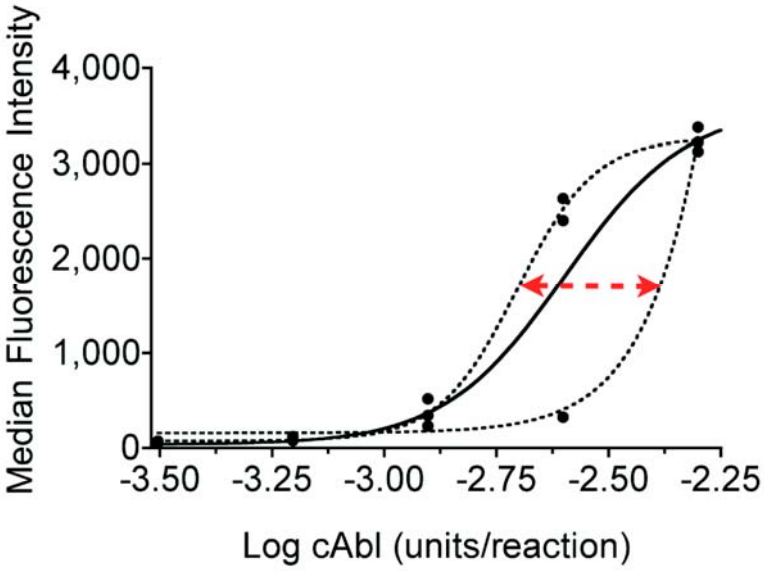

Supplementary Figure 1. Immobilized Abltide was phosphorylated by purified recombinant Abl kinase and labeled with biotinylated 4G10 and phycoerythrin-conjugated streptavidin. The median fluorescence intensity from a sampling of 100 beads per well revealed dispersion between triplicate wells. This dispersion influenced the slope and EC_{50} of the best-fit sigmoidal curve. A dashed red line with arrows emphasizes the difference in EC_{50} values that can result from either discarding or over-emphasizing outliers. Two dashed sigmoidal curves display EC_{50} values of 0.038 and 0.182 enzyme units per mL depending on whether one well from a set of triplicates is discarded or over-emphasized. The best-fit curve that includes all three data points displays an EC_{50} value of 0.05 enzyme units/mL. There is a minimum difference of 35% between EC_{50} values derived from curves that include or exclude an outlier. To allow better judgment concerning outlier exclusion, a more descriptive analysis of the data is provided by the mean fluorescence intensity per bead population and a confidence interval that accounts for the number of beads sampled.

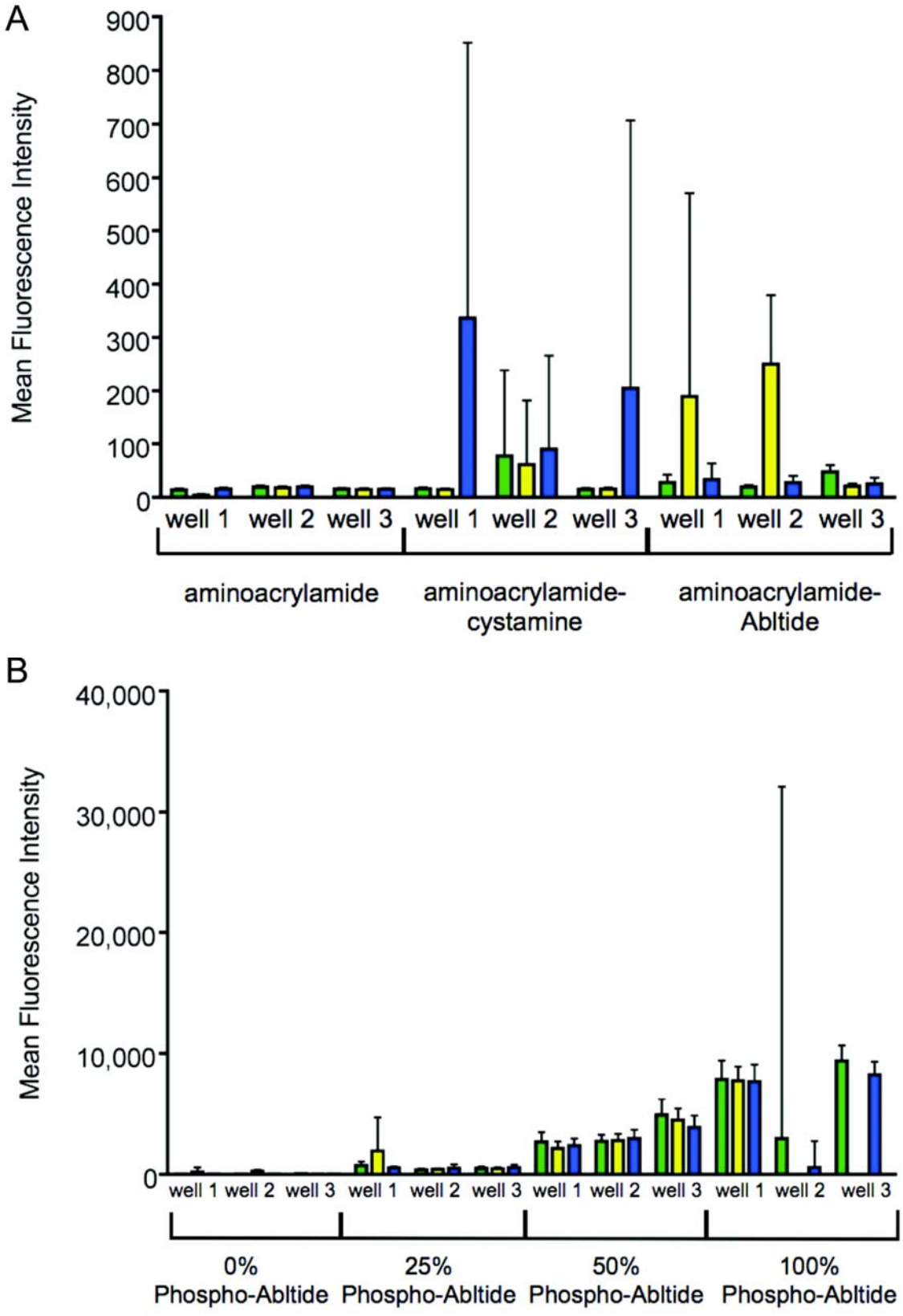
A
Mean Fluorescence Intensity
900
800
700
600
500
400
300
200
100
0
well 1 well 2 well 3 well 1 well 2 well 3 well 1 well 2 well 3
aminoacrylamide
aminoacrylamide-cystamine
aminoacrylamide-Abltide
B
Mean Fluorescence Intensity
40,000
30,000
20,000
10,000
0
well 1 well 2 well 3 well 1 well 2 well 3 well 1 well 2 well 3 well 1 well 2 well 3
0% Phospho-Abltide
25% Phospho-Abltide
50% Phospho-Abltide
100% Phospho-Abltide

Supplementary Figure 2. Sources of variability and their effects on data distributions are demonstrated via replicate wells and replicate runs of the same wells. Background fluorescence is compared with differentially conjugated beads to show low non-specific binding to un-phosphorylated peptide substrate. Synthetic phospho-standards are arranged in separate wells, as in traditional calibration curves, to demonstrate the range in fluorescence intensities obtained from separate wells and thereby strongly support well-specific internal standards for accurate measurement, independent of plate-to-plate and run-to-run fluctuations. Figures **A** and **B** demonstrate the variability of fluorescence measurements. This data confirms the need for well-specific internal standards. For each figure, we prepared a 96-well plate and ran it on the BioPlex 200 three consecutive times. The only change to the plate between runs was the added Luminex running buffer from the BioPlex 200 upon replacement of the sampled beads. Green, yellow and blue columns show separate measurements for runs 1, 2, and 3 per well in arbitrary units of raw fluorescence intensity. While some wells had consistent values across three runs, others showed large variability from run to run. Error bars represent the 99% confidence interval around the mean and are a function of the number of beads sampled per run. This variability between runs and between wells undermines the effectiveness of an external standard but does not affect the validity of an internal standard. **A,** testing separate background values, including an acrylamide-coated bead surface, a cystamine-acrylamide-coated surface, and a peptide-acrylamide-coated surface, we confirmed low non-specific antibody binding for chemically modified beads. For reference, un-conjugated beads demonstrated a mean fluorescence intensity of 4 arbitrary units. In contrast, un-phosphorylated peptide-conjugated beads demonstrate approximately 30 arbitrary units of fluorescence intensity. **B,** the mean fluorescence intensity increased well beyond background values as a result of the specific interaction of anti-phosphotyrosine antibodies with phosphorylated standards immobilized on beads.

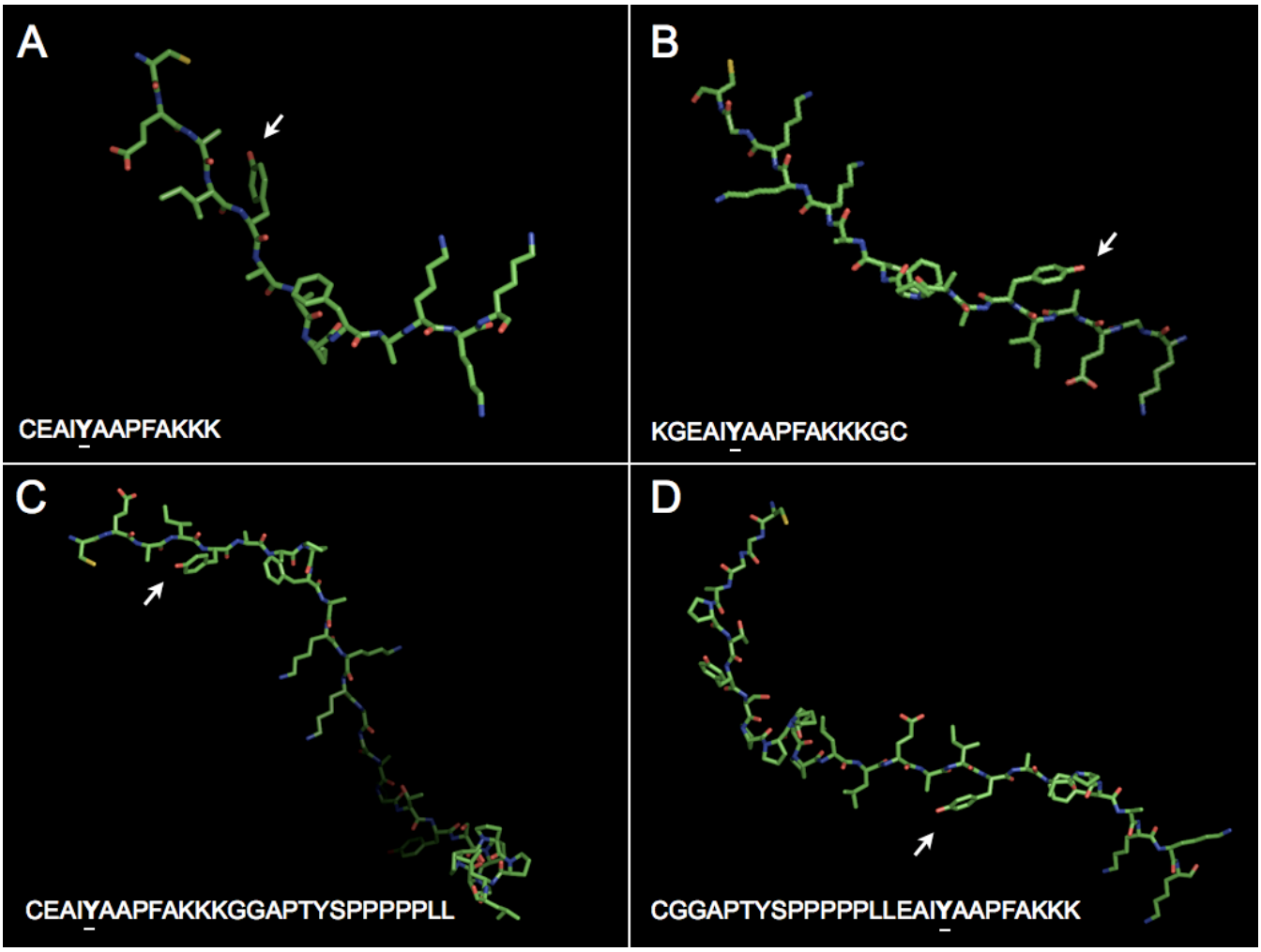

Supplementary Figure 3. Peptides were modeled by PyMOL (Delano Scientific, Palo Alto, CA; http://www.pymol.org) to investigate the effects of substrate orientation relative to the site of immobilization for four variants of the Abltide substrate. Figures A and B demonstrate the effects of reversing the site of Abltide immobilization from the amino-terminus to the carboxyl-terminus. Figures C and D demonstrate the effect of including p40 in tandem with Abltide either distal (C) or proximal (D) to the site of immobilization. Figures B and D suggest that the tyrosine is more accessible to phosphorylation when Abltide is immobilized via its carboxyl-terminus or when p40 is inserted distal to the immobilization site. All substrates are oriented so that the cysteine residue that is covalently immobilized to acrylamide-coated Luminex beads is in the upper left hand corner. Carbon atoms are represented in green, nitrogen in blue, oxygen in red, and sulfur in yellow. Hydrogen atoms are not shown. White arrows indicate the location of the substrate tyrosine that is

phosphorylated. Peptide sequences are noted at the lower left hand corner of each figure, and the substrate tyrosine is highlighted by an underscore.

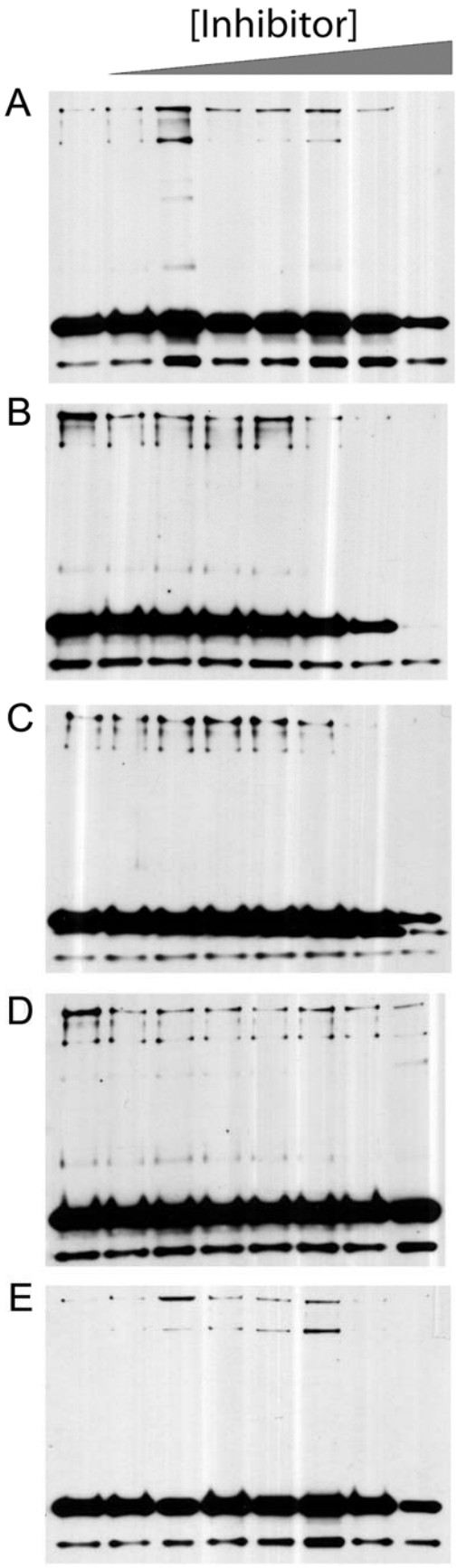

Supplementary Figure 4. A multiplexed Western blot was performed on lysates following the treatment of cells with inhibitors in culture. The phosphorylation of Bcr-Abl, Abl, and CrkL are monitored simultaneously relative to eIF4e, a control for the equal loading of lanes. Relative decreases in protein phosphorylation states indicate the inhibition of kinase activity. Confluent cells were treated in culture with (**A**) imatinib, (**B**) dasatinib, (**C**) PD166326, (**D**) PD173955, or (**E**) DV2-273. Inhibitors were serially diluted ten-fold in DMSO, for final concentrations ranging from 10^{-4} to 10^{2} nM (μM for imatinib). Untreated controls are positioned at the far left. The PathScan Bcr/Abl Activity Assay (Cell Signaling Technologies) was used to query the activation state of Abl and Bcr-Abl, as well as the phosphorylation of the Abl kinase substrate CrkL, in lysates prepared in conical tubes from cells treated with inhibitors in culture.

The major bands in each gel from top to bottom represent phosphorylated Bcr-Abl, phosphorylated Abl, phosphorylated CrkL, and eIF4e, which is intended as a control for equal lane loading. Stat5a does not appear in these exposures. Only one representative exposure is shown. These results suggest that the phosphorylation of Bcr-Abl is inhibited in cells by imatinib with an IC_{50} near 10 μM, by dasatinib with an IC_{50} between 0.1 and 1 nM, by PD166326 with an IC_{50} near 1 nM, by PD173955 with an IC_{50} near 100 nM, and by DV2-273 with an IC_{50} between 1 and 10 nM. Although this figure does not allow the comparison between differences in CrkL phosphorylation, separate exposures indicate that a ten-fold

increase in inhibitor concentration is required to see a comparable decrease in CrkL phosphorylation, compared to Bcr-Abl phosphorylation.

Previous comparisons demonstrate that IC_{50} values between results from our bead-based activity assay and Western blots for Bcr-Abl phosphorylation do not agree exactly, partly due to differences in the detection of kinase activation state versus activity, as well as basic differences in technique. In general, these results fall within intermediary values of those tested by our bead-based assay. Although results are not directly comparable due to differences in sample preparation, the combination of bead-based and Western detection techniques provides an estimate for the inhibition of Bcr-Abl following the treatment of cells in culture.